TARGETED COMPLEXES BASED ON UPCONVERSION NANOPARTICLES FOR IMAGING IN THE FIRST AND SECOND OPTICAL TISSUE TRANSPARENCY WINDOW

E.L. Guryev[*1], *V.A. Sukhova* [1], *A.V. Yudintsev* [1], *A.B. Kostyk* [1], *A.V. Lubeshkin* [2], *J. Chen* [3], *A.V. Zvyagin* [1, 4, 5]

[1] Institute of Biology and Biomedicine, Lobachevsky State University of Nizhny Novgorod, Nizhny Novgorod, 603950, Russia;
[2] Federal Scientific Research Center "Crystallography and Photonics", Russian Academy of Sciences, 119333 Moscow, Russia;
[3] Department of Orthopaedic Sports Medicine, Huashan Hospital, Fudan University, 200040, Shanghai, China;
[4] The Institute of Molecular Medicine, I.M. Sechenov First Moscow State Medical University, 119991 Moscow, Russia;
[5] ARC Centre of Excellence «Nanoscale BioPhotonics», Department of Physics and Astronomy, Macquarie University, Sydney 2109, Australia.

[*] Corresponding author: eguryev@ibbm.unn.ru

Abstract. Achieving both deep penetration of photons into biological tissue and highly sensitive recording of optical probes' response are the key goals of non-invasive optical imaging. In comparison with the traditional fluorescence imaging in the visible (400–700 nm) and near-infrared (700–900 nm) regions, optical fluorescence imaging in the second optical tissue transparency window (1000–2300 nm) demonstrates low photon scattering, deeper penetration into the tissues and lower autofluorescence. In the present study, biocompatible upconversion nanoparticles with different contents of doping lanthanides, capable of luminescence in the visible and short-wave IR regions, were obtained and characterized. Also, targeted complexes based on Gd-containing nanophosphors were obtained as potential contrast agents for magnetic resonance imaging. Selective binding of targeted complexes to the surface of tumor cells expressing the HER2 receptor was shown.

Keywords: Upconversion nanoparticles, short-wave infrared optical imaging, targeted complexes.

List of Abbreviations

CT – computed tomography
DARPin – designed ankyrin repeat protein
DLS – dynamic light scattering
DMF – Dimethylformamide
EDC – 1- ethyl-3-(3-dimethylaminopropyl) carbodiimide IR – infrared
FTT – photothermal therapy
HER2 – human epidermal growth factor receptor 2
LoPE – low immunogenic pseudomonas exotoxin
MRI – magnetic resonance imaging
NIR – near-infrared radiation
nm – nanometer
PBS – phosphate buffered saline
PDI – polydispersity index
PL – photoluminescence
SWIR – short wavelength IR region
sulfo-NHS – N-hydroxysulfosuccinimide
TEM – transmission electron microscope
UCNP – upconversion nanoparticles

Introduction

The development of agents for multimodal imaging of biological objects, including individual cells, is an actively developing area of modern biomedicine. The new paradigm of creating multifunctional agents «one for everything», based on the multimodality of the core, allows one to overcome the barrier of the complexity of multicomponent agents created on the principle of «all in one». Successful examples of the new strategy are the majority of inorganic nanoparticles with imaging and therapeutic properties: magnetic nanoparticles for thermotherapy and magnetic resonance imaging (MRI) (Jordan et al., 2006), gold nanoparticles for radiation therapy and computed tomography (CT) (Huang et al., 2011), gold nanorods for photothermal therapy (FTT) and CT contrast enhancement (von Maltzahn et al., 2009), porphisomes for fluorescent and optoacoustic imaging and photodynamic therapy, etc.

(Charron et al., 2015). The most promising strategy seems to be a hybrid approach aimed at reducing the number of components by multiplying the functions not only of the core itself but also of the attached modules. In particular, the use of photoluminescent nanomaterials as a core and bifunctional agents (for example, gold nanoparticles for diagnostics and FTT, recombinant toxins for targeted therapy) as additional modules.

Ideally, imaging technology should be fast, highly sensitive, deeply penetrating, and capable of long-term observation. MRI provides a spatial resolution of anatomical structures and also provides functional information about soft tissues, but its sensitivity is relatively low. Typically, the contrast based on the amount of water is used only to create anatomical images where water content is important in various tissues. The use of compounds based on Gd3+ as an additional contrast provides high sensitivity, resolution, specificity and the possibility of studies in dynamics. Contrast agents for MRI based on Gd3+ are widely used in clinical practice and experimental studies. However, such agents are poorly absorbed by cells, therefore, to enhance their absorption, the binding of a contrast agent with peptides that facilitate transport across the cell membrane or transfecting agents is used (Rudelius et al., 2003).

Compared to other approaches, the optical imaging of cells is a low cost, rapidity of execution, the lack of radiation needed and relatively high sensitivity (Sabapathy et al., 2015). On the other hand, the use of fluorescence imaging techniques is limited to short wavelengths, which does not allow imaging of objects such as bones and skin (Shichinohe et al., 2004). This limitation can be overcome by photoluminescent nanoparticles with emission maxima in the near-IR region.

Water, hemoglobin, melanin, and lipids act as the main light absorbers, while tissue composition and morphology affect light scattering. Near-infrared radiation (NIR, 700–1000 nm) is weaker absorbed by tissue components than visible light, which allows deeper imaging in the first "transparency window" of biological tissue. However, it has recently been shown that a second "transparency window" located in the short wavelength IR region (SWIR, 1000-2300 nm) has relatively low tissue absorption and autofluorescence, which are comparable in magnitude to NIR. At the same time, the losses associated with scattering are 1000 times less, which opens up opportunities for an unprecedented improvement in the depth and resolution of optical probe detection.

Recent studies have shown that upconversion nanoparticles (UCNP) containing lanthanide ions are capable of luminescence in the SWIR with a large Stokes shift when excited with low-intensity light with a wavelength of 980 nm (Tan et al., 2009). Traditionally, bioimaging using UCNP has been based on their anti-Stokes luminescence in the visible region of the spectrum. Relatively recent studies have revealed the potential of UCNP as probes for diagnosing pathologies and bioimaging in the second transparency window of biological tissue (Naczynski et al., 2013).

In the present study, upconversion nanoparticles (UCNP) doped with ytterbium, erbium, thulium and gadolinium ions and exhibiting photoluminescence in the visible and IR spectral regions were obtained and characterized. UCNPs doped with Tm and Gd ions, intended for bimodal IR and MR imaging, were functionalized with the targeted protein DARPin-LoPE. The specific binding of the obtained target complexes with cells expressing the HER2 receptor was shown.

Materials and Methods

Obtaining of UCNP. Core/shell UCNP with composition NaY0.78Yb0.20Er0.02F4\NaYF4 (UCNP (2mol%Er)), NaY0.77Yb0.20Er0.03F4\NaYF4 (UCNP (3mol%Er)) and UCNP with composition NaY0,695F4Yb0,2Tm0,08Gd0,025 (UCNP (Tm,Gd)) were synthesized by the solvothermal decomposition of precursors as described earlier (Guryev et al., 2020).

Coating of UCNP with a shell of polyacrylic acid (PAA) molecules was carried out by the ligand exchange method. Oleic acid ligands were removed from UCNP surface using nitrosonium tetrafluoroborate (NOBF4). 10 ml of NOBF4 solution was added to 10 μl of UCNP suspension in cyclohexane (5 mg/ml), the mixture was incubated 12 h with stirring in a sealed flask. The mixture was centrifuged, the supernatant was removed, UCNP-NOBF4 was dispersed in a mixture of dimethylformamide (DMF), toluene and cyclohexane. The mixture was centrifuged, the supernatant was removed, UCNP-NOBF4 was dispersed in 5 ml DMF, then 5 ml of PAA solution in DMF (30 mg/ml) was added. The mixture was incubated for 3 h in a sealed flask at 80°C with stirring. UCNP-PAA was collected by centrifugation and washed three times with ethanol and three times with deionized water.

Characterization of UCNP. UCNP images were obtained using a CM10 transmission electron microscope (Philips, Netherlands) at a voltage of 100 kV. The hydrodynamic diameter of particles was measured by dynamic light scattering using the Zetasizer Nano ZS system (Malvern Instruments Ltd., UK).

The PL emission spectrum of UCNP in the range of 400-830 nm was obtained using a CM 2203 spectrofluorimeter (SOLAR, Belarus). To excite the PL an external semiconductor laser module ATC-C4000-200AMF-980-5-F200 (Semiconductor devices, Russia) with a wavelength of 978 nm was used.

The PL spectra of UCNP in the IR spectral region were studied using a laboratory spectroscopic setup. An ATC-C4000-200AMF-980-5-F200 semiconductor laser module with a wavelength of 978 nm was used as a source of exciting radiation. The radiation of the laser diode was collected in a multimode fiber (diameter 200 μm) connected to the collimator F280SMA-980 (ThorLabs, USA), collimated radiation with a diameter of 4 mm at an angle of 45 ° was directed to a quartz cuvette (10×10×44 mm), with a suspension of the sample under study, where the UCNP PL was excited. This illumination scheme was used to minimize the fraction of scattered laser radiation directed towards the monochromator's entrance slit. The UCNP PL was projected onto the entrance slit of the monochromator using a collecting lens. A mechanical interrupter SR540 (Stanford Research Systems, USA), which set the reference signal for the lock-in amplifier SR810 (Stanford Research Systems, USA) and a cut-off filter LP02-980RE (Semrock, USA), which blocked the scattered radiation of the diode laser, were installed in front of the entrance slit of the monochromator. Using an SP-150 monochromator lattice (Acton Research, USA) 300 lines/mm, a narrow portion of the UCNP PL spectrum in the range from 1000 to 1700 nm was sequentially distinguished. The selected part of the spectrum was detected using an InGaAs detector (Acton Research, USA), PL signal was processed by a lock-in amplifier, digitized, and stored on a personal computer.

To study the penetration depth of UCNP PL through biological tissues, layers of muscle tissue with a thickness of 1 to 4 mm were placed close to the cuvette with the UCNP suspension so that both exciting radiation in the direction of the UCNP sample and the UCNP PL in the direction of the detector passed through them.

Assembly of targeted complexes. Targeted protein DARPin-LoPE was obtained as previously described (Guryev et al., 2020). UCNP-PAA with functional carboxyl groups were covalently linked to targeted protein molecules using a zero-length linker 1-ethyl-3-(3-dimethylaminopropyl)carbodiimide (EDC) in the presence of N-hydroxysulfosuccinimide (sulfo-NHS). Carboxyl groups of UCNP-PAA were activated with EDC/sulfo-NHS in MES buffer (100 mM MES, 150 mM NaCl, pH 6.0), the suspension was washed with phosphate buffered saline (PBS), DARPin-LoPE protein solution was added in a ratio of 2:1 protein:UCNP (w:w), the mixture was incubated for 2 h with stirring. The assembled complexes were washed three times with PBS to remove unbound protein molecules. The concentration of the protein component in the targeted complexes was determined by the BCA method.

Investigation of the interaction of UCNP and targeted complexes with tumor cells. To study the interaction of targeted complexes with the HER2 receptor on the cell surface, we used a culture of human ovarian carcinoma cells SKOVip, overexpressing the HER2 receptor on the surface. Human epidermoid carcinoma cells A431 were used as control (HER2–) cells. SKOVip and A431 cells were cultured in McCoy's medium (HyClone, USA) supplemented with L-glutamine and 10% fetal bovine serum (HyClone, USA). The cells were seeded onto coverslips placed in the wells of a 6-well plate at a concentration of 2.5x105 cells/ml and incubated for 24 h at 37°C and 5% CO2. The cell medium was replaced with PBS, and a suspension of targeted complexes or UCNP was added to a concentration of 1 μg/ml. To prevent endocytosis of nanoparticles, cells were incubated for 1 h at 4°C. The cells were washed with PBS and fixed with 4% formaldehyde solution for 30 min in the dark. Formaldehyde was removed, cells were washed 3 times with PBS and 1 time with deionized water. The coverslips were removed from the wells of the plate, dried, placed in a drop of glycerol on the glass slides and sealed. The binding of particles to the cell surface was assessed by confocal laser fluorescence microscopy using an Axio Observer Z1 LSM-710 DUO NLO microscope (Carl Zeiss, Германия). Pulsed PL excitation was performed with a Chameleon Vision II titanium-sapphire laser (Coherent, USA) at a wavelength of 980 nm with a repetition rate of 80 MHz and a pulse duration of ~140 fs. The UCNP PL signal was recorded using a 32-channel photodetector in the spectral ranges 446-486 nm and 768-850 nm.

Results

Synthesis and characterization of UCNP-Er. UCNP doped with lanthanide ions were used as visualizing agents in this study. UCNPs possess unique photoluminescent properties and photochemical stability; therefore, they have advantages over other fluorophores and are widely used as effective markers for deep bioimaging.

For doping the NaYF4 matrix, we used ions of trivalent lanthanides – ytterbium (Yb3+) and erbium (Er3+). The percentage of ytterbium and erbium was selected based on the available data on the photoluminescence (PL) intensity of various UCNPs in the range 1000-1700 nm. Core/shell UCNP (2mol%Er) and UCNP (3mol%Er) were synthesized by the solvothermal decomposition with additional heat treatment to transfer them from the α-cubic phase to a more stable β-hexagonal phase (Fig. 1 A, B). The NaYF4 shell additionally stabilizes the core of UCNP (2mol%Er) and UCNP (3mol%Er) and increases the radiation conversion efficiency.

UCNP (2 mol% Er) and UCNP (3 mol% Er) had bright PL with emission maxima in the green (at a wavelength of 541 nm) and red (at a wavelength of 658 nm) upon excitation at 978 nm (Fig. 1 C, D, E). The peak of the PL emission in the IR region of Erbium-doped UCNP is in the region of 1525 nm, and its value is proportional to the intensity of the exciting radiation at 978 nm (Fig. 1 F, G).

According to transmission electron microscopy (TEM), the particle size of UCNP (2mol%Er) and UCNP (3mol%Er) was 31.8±4.1 nm and 29.2±3.2 nm, respectively (mean values±standard deviation). Nanoparticles of this size can be successfully used in in vivo experiments without the risk of rapid elimination from the body of laboratory animals.

To study the penetration depth of UCNP PL through biological tissues, layers of muscle tissue with a thickness of 1 to 4 mm were placed close to the cuvette with the UCNP suspension so that both exciting radiation in the direction of the UCNP sample and the UCNP PL in the direction of the detector passed through them. The PL signal was recorded in the range of 1450–1650 nm (Fig. 2). The PL signal from UCNP (2mol%Er) was recorded through a 2 mm tissue layer. At a greater thickness, a pronounced signal was not observed. In the case of UCNP (3mol%Er), the PL intensity was significantly higher, and the PL signal was recorded up to a tissue thickness of 3 mm.

Synthesis and characterization of UCNP-Tm,Gd

To investigate the possibilities of bimodal imaging, ytterbium, thulium, and gadolinium

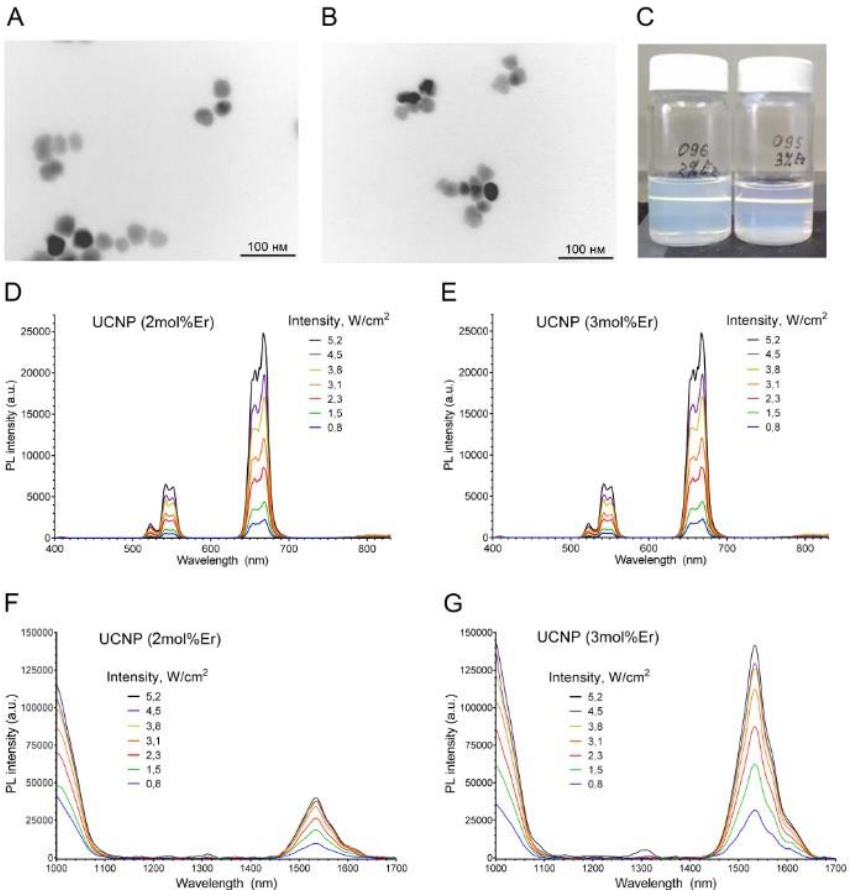

Fig. 1. A, B – TEM images of UCNP (2 mol% Er) (A) and UCNP (3 mol% Er) (B) with a magnification of x180000; C - suspensions of UCNP (2 mol% Er) and UCNP (3 mol% Er) illuminated by a laser with a wavelength of 980 nm; D, E – PL emission spectra of UCNP (2mol%Er) (D) and UCNP (3mol%Er) (E) in the visible region of the spectrum upon excitation at 978 nm with an intensity of 0.8 to 5.2 W/cm^2; F, G – PL emission spectra of UCNP (2 mol% Er) (E) and UCNP (3 mol% Er) (G) in the IR spectral region in the range 1000-1700 nm upon excitation at 978 nm with an intensity of 0.8 to 5.2 W/cm^2

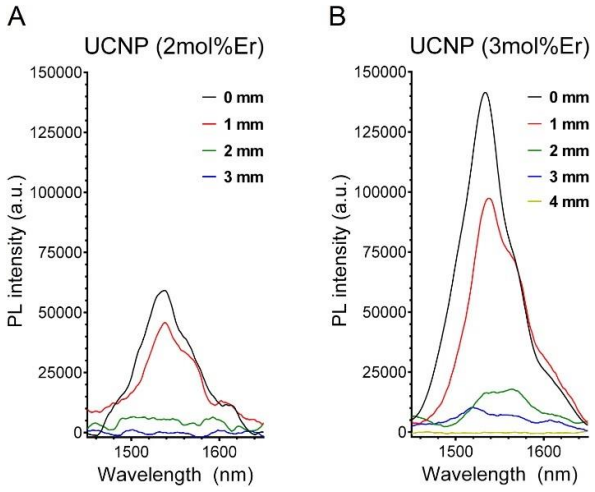

Fig. 2. Penetration depth of PL of UCNP (2mol%Er) (A) and UCNP (3mol%Er) (B) through biological tissues of various thicknesses upon excitation at 978 nm

nents. Thulium doping ions provides a UCNP with bright photoluminescence in the near-infrared region, which is a valuable feature for bioimaging applications. The inclusion of gadolinium ions in UCNP will make it possible to carry out MR imaging of biological objects in combination with optical imaging in the IR region.

UCNP (Tm, Gd) were synthesized by solvatothermal decomposition. According to TEM data, the particle size was 26.5 ± 1.1 nm (Fig. 3A), which is optimal for biomedical applications. UCNPs doped with ytterbium and thulium ions exhibit PL maxima in the visible region (474 nm), near IR (801 nm) (Fig. 3B, C). The brightest is the UCNP (Tm, Gd) PL band in the near-IR region (801 nm) upon excitation at 978 nm. In this case, both the exciting radiation and the PL signal of UCNP are able to penetrate deeply through biological tissues.

UCNP synthesis is usually carried out in non-polar organic solvents, which makes them hydrophobic and limits their biocompatibility. Consequently, a necessary step is the modification and functionalization of their surfaces to make them stable in aqueous solutions, biocompatible and provide them with reactive groups for conjugation with biomolecules. Ligand exchange is one of the commonly used methods for modifying the UCNP surface. It consists in replacing the original hydrophobic ligands with hydrophilic ones. For this purpose, various compounds are actively used, in particular, polyacrylic acid (PAA). This approach can reduce the PL quantum yield, but it helps to maintain the size and colloidal stability of nanoparticles.

Coating of UCNP (Tm, Gd) with a shell of PAA molecules was carried out by the ligand exchange method, while the ligands of oleic acid on the UCNP surface were removed using nitrosonium tetrafluoroborate (NOBF4). As a result, a suspension of UCNP (Tm, Gd) coated with a biocompatible PAA shell with a hydrodynamic diameter of 53.1 ± 8.5 nm was obtained (Fig. 4A); the value of the polydispersity index (PDI) was 0.328. The hydrodynamic diameter of UCNP-PAA is larger than the TEM-determined "dry" particle size due to the formation of a hydration shell around the particles in an aqueous medium. The data obtained make it possible to consider UCNP-PAA to be fairly uniform in size and suitable for biomedical applications.

Preparation of targeted complexes. UCNP-PAA particles by themselves do not possess targeting properties and can only be used for non-specific labeling of cells or tissues. The functional carboxyl groups of PAA on the surface of the particles are suitable for attaching to them various modules that have an affinity for a particular biological target (Fig. 5). In the present study, human epidermal growth factor receptor 2 (HER2) was used as a target. The HER2 receptor's overexpression is common in many types of epithelial tumors, such as breast, ovarian, bladder, salivary, endometrial, pancreatic, and non-small cell lung cancer.

The targeted protein DARPin-LoPE was used as a targeting module, which includes the targeting scaffold DARPin - designed ankyrin repeat protein, which specifically binds to the HER2 receptor on the cell surface [Sokolova et al., 2019]. The complexes were assembled by covalent chemical conjugation of PAA carboxyl groups with protein amino groups using a zero-length linker 1-ethyl-3-(3-dimethylaminopropyl)carbodiimide (EDC) in the presence of N-hydroxysulfosuccinimide (sulfo-NHS) (Fig. 5). This technology allows the formation of stable amide bonds between modules and avoids the destruction of the complex, as in the case of non-covalent assembly.

As a result, a suspension of targeted UCNP-PAA-DARPin-LoPE complexes with an average hydrodynamic particles diameter of 88.7±14.4 nm (Fig. 4B) and PDI value of 0.308 was obtained. The increase in the average particle size is explained by the attachment of protein molecules and the formation of additional hydration shells. The concentration of the target protein in the complexes was 1.239 mg/ml at a UCNP-PAA concentration of 1 mg/ml, which corresponds to ~730 protein molecules per particle. The properties of the targeted complexes make it possible to count on their effective use as specific imaging agents.

Study of the interaction of UCNP-PAA and targeted complexes with tumor cells in vitro.

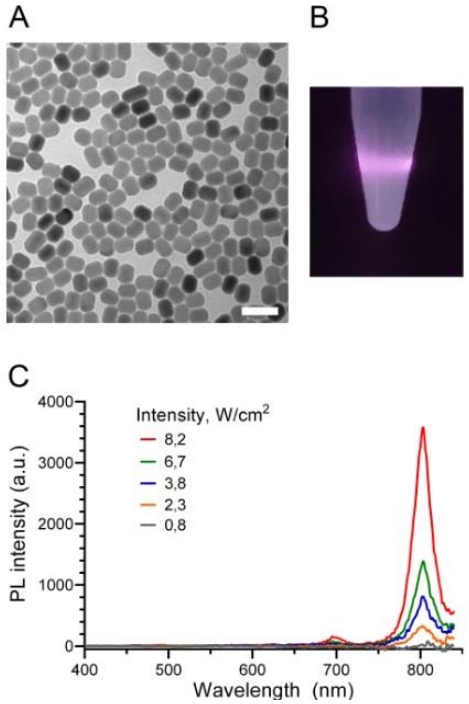

Fig. 3. Properties of UCNP (Tm,Gd). A – TEM image of UCNP (Tm,Gd) with a magnification of x130000; scale bar 50 nm; B – UCNP (Tm,Gd) suspension under irradiation at 978 nm; C – PL spectrum of UCNP (Tm,Gd) in the visible and IR regions upon excitation at 978 nm with an intensity of 0.8 to 8.2 W/cm^2

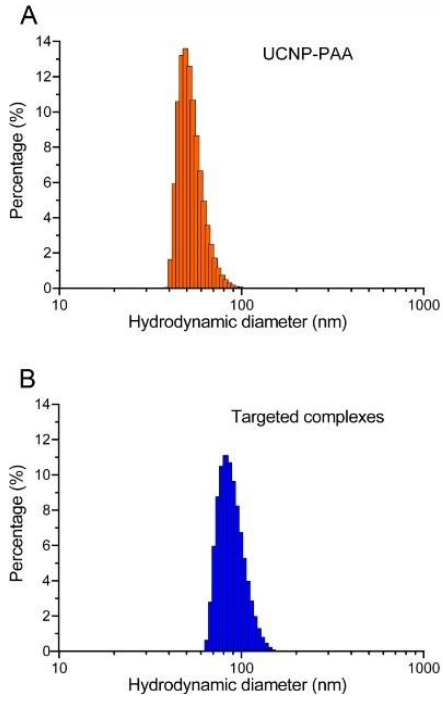

Fig. 4. Hydrodynamic diameter distribution of UCNP-PAA (A) and targeted complexes (B)

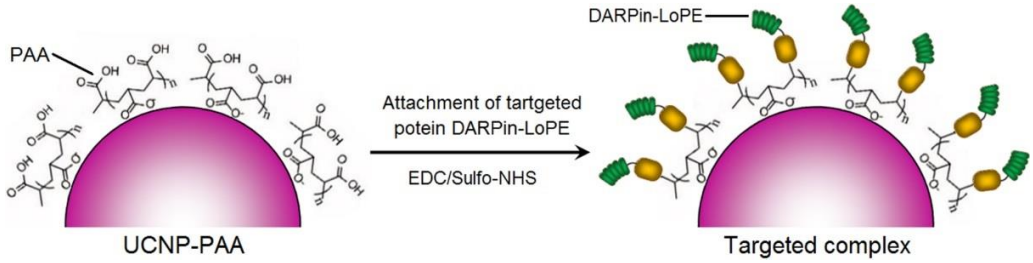

Fig. 5. Scheme of assembly of target complexes based on UCNP and targeted protein DARPin-LoPE

One of the main properties of the obtained target complexes is the possibility of specific visualization of target cells. To investigate the possibility of specific visualization, the following cell lines were used: human ovarian carcinoma cells SKOVip, overexpressing the HER2 receptor on the surface, and human epidermoid carcinoma A431 cells with no expression of the HER2 receptor. The targeted protein DARPin-LoPE attached to UCNP-PAA particles imparts targeted properties to the entire complex, while the PL properties of UCNP allow visualization of biological objects using fluorescence microscopy and fluorescence imaging.

Cells of both lines were incubated for 1 h in the presence of targeted complexes and UCNP-PAA, washed, fixed, and examined using confocal laser fluorescence microscopy. The obtained micrographs of SKOVip (HER2+) cells after incubation with targeted complexes

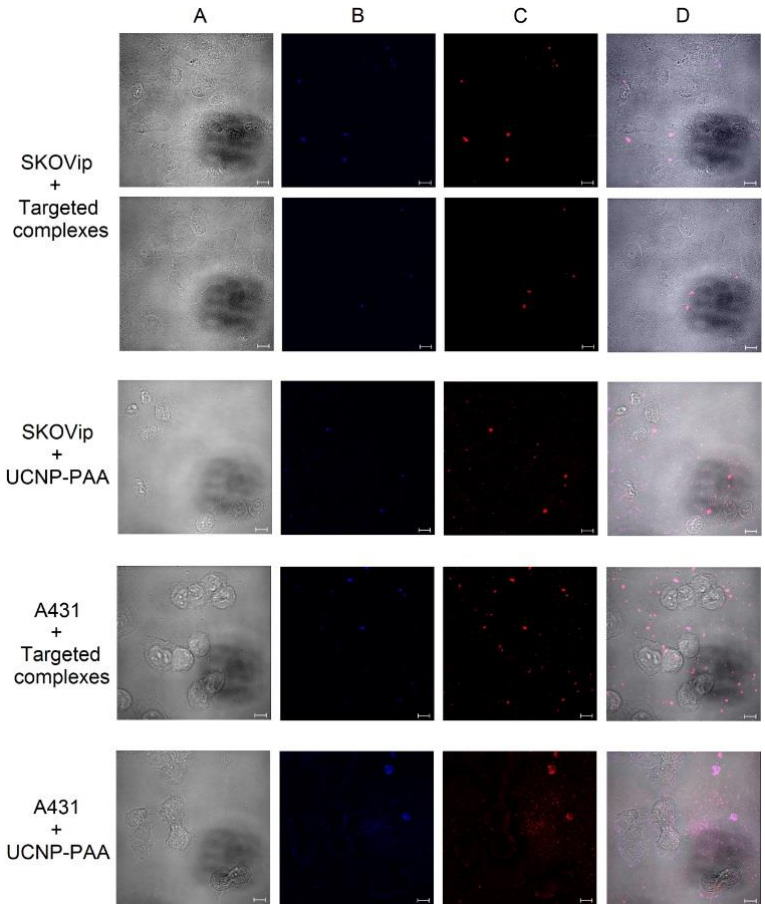

Fig. 6. Micrographs obtained by confocal fluorescence microscopy: SKOVip (HER2+) and A431 (HER2–) cells incubated for 1 h with targeted complexes and UCNP-PAA. A – bright-field image of cells; B – PL signal in the range 446-486 nm, C – PL signal in the range 768-850 nm; D - overlay of images A, B and C. Scale bar 10 μm

clearly show the accumulation of particles on the cell membrane (Fig. 6). On micrographs of A431 (HER2–) cells after incubation with targeted complexes, the accumulation of particles on the cell membrane is not pronounced, the particles are arranged chaotically (Fig. 6). After incubation of SKOVip (HER2+) and A431 (HER2–) cells with non-targeted UCNP-PAA particles, no specific accumulation of particles was observed on the cell surface membrane (Fig. 6). Thus, microscopic data indicate the specific binding of the obtained target complexes to the surface of cells expressing the HER2 receptor.

Discussion

The detection efficiency of bioimaging probes is determined by the intensity of their photoluminescence, the length of the optical path through tissues and the volumetric distribution of energy, which is due to the absorbing and scattering properties of biological media and tissues. UCNP have a set of photophysical properties that give them advantages over other fluorescent probes. Especially valuable properties are the possibility of PL excitation by low-intensity IR light and the presence of narrow PL emission peaks not only in the visible, but also in the near IR and shortwave IR spectral regions (Naczynski et al., 2013). Doping UCNP's matrix with Tm3+ and Er3+ ions makes it possible to obtain UCNP with PL in the region of 800 nm and 1525 nm, falling into the biological tissue transparency window I and II, respectively. Depending on the application, this offers the opportunity to take advantage of one option or another, including low tissue autofluorescence, reduced light absorption and scattering.

The UCNP and targeted complexes developed in this study fully correspond to the current strategy of creating multifunctional agents. The wide possibilities of fluorescence imaging in the IR region in combination with highly sensitive magnetic resonance (MR) imaging allow us to count on the advantages of both approaches. The obtained targeted complexes have an optimal size for delivery to target tissues and cells via both passive and active pathways. Modification of the surface gives them biocompatibility and colloidal stability. The modular design of the complexes and the choice of UCNP dopants (not limited to erbium, thulium and gadolinium) make it possible to obtain targeted complexes that are specific to any of a variety of biological targets and with the desired imaging properties. Recombinant proteins with a given specificity can include not only targeting but also visualizing (fluorescent) or toxic modules, which further expands the functionality of the complexes without complicating their structure. The targeted protein DARPin-LoPE used in this study is capable of exerting a specific toxic effect on HER2-overexpressing tumor cells (Sokolova et al., 2019) due to the presence of a targeting and toxic module in its structure. Conjugation of UCNP with such bifunctional protein molecules made it possible to obtain multifunctional complexes capable of specifically interacting with a certain type of tumor cells. Due to the combination of visualizing and targeted properties, the developed complexes are of undoubted interest as promising agents for multimodal imaging.

Acknowledgements

This research was supported by the RFBR and NSFC according to the research project № 19-54-53025.

References

CHARRON D.M., CHEN J. & ZHENG G. (2015): Theranostic Lipid Nanoparticles for Cancer Medicine. In: (Nanotechnology-Based Precision Tools for the Detection and Treatment of Cancer // Cancer Treatment and Research (Eds MIRKIN C., MEADE T., PETROSKO S. & STEGH A.), pp103-127, V 166, Springer.

HUANG P., BAO L., ZHANG C., LIN J., LUO T., YANG D., HE M., LI Z., GAO G., GAO B., FU S. & CUI D. (2011): Folic acid-conjugated silica modifiedgold nanorods for X-ray/CT imaging-guideddual-mode radiation and photo-thermal therapy. Biomaterials. 32, 9796–9809.

GURYEV E.L., SMYSHLYAEVA A.S., SHILYAGINA N.Y., SOKOLOVA E.A., SHANWAR S., KOSTYUK A.B., LYUBESHKIN A.V., SCHULGA A.A., KONOVALOVA E.V., LIN Q., ROY I., BALALAEVA I.V., DEYEV S.M. & ZVYAGIN A.V. (2020): UCNP-based Photoluminescent Nanomedicines for Targeted Imaging and Theranostics of Cancer. Molecules, 25(18), 4302.

JORDAN A., SCHOLZ R., MAIER-HAUFF K. VAN LANDEGHEM F.K., WALDOEFNER N., TEICHGRAEBER U., PINKERNELLE J., BRUHN H., NEUMANN F., THIESEN B., VON DEIMLING A. & FELIX R. (2006): The effect of thermotherapyusing magnetic nanoparticles on rat malignantglioma. J Neurooncol. 78, 7–14.

NACZYNSKI, D. J., TAN M.C., ZEVON M., WALL B., KOHL J., KULESA A., CHEN S., ROTH C.M., RIMAN R.E. & MOGHE P.V. (2013): Rare-earth-doped biological composites as in vivo shortwave infrared reporters. Nat. Commun. 4, 2199.

RUDELIUS M., DALDRUP-LINK H.E., HEINZMANN U., PIONTEK G., SETTLES M., LINK T.M. & SCHLEGEL J. (2003): Highly efficient paramagnetic labelling of embryonic and neuronal stem cells. Eur. J. of Nuc. Med. and Mol. Imag. 30(7), 1038–1044.

SABAPATHY V., MENTAM J., JACOB P.M. & KUMAR S. (2015): Noninvasive optical imaging and in vivo cell tracking of indocyanine green labeled human stem cells transplanted at superficial orin-depth tissue of SCID mice. Stem Cells International. 2015, 606415.

SHICHINOHE H., KURODA S., LEE J.-B., NISHIMURA G., YANO S., SEKI T., IKEDA J., TAMURA M. & IWASAKI Y. (2004): In vivo tracking of bone marrow stromal cells transplanted into mice cerebral infarct by fluorescence optical imaging. Brain Research. Brain Research Protocols. 13(3), 166–175.

SOKOLOVA E.A., SHILOVA O.N., KISELEVA D.V., SCHULGA A.A., BALALAEVA I.V. & DEYEV S.M. (2019): HER2-Specific Targeted Toxin DARPin-LoPE: Immunogenicity and Antitumor Effect on Intraperitoneal Ovarian Cancer Xenograft Model. Int. J. Mol. Sci., 20(10), 2399.

TAN M.C., KUMAR G.A., RIMAN R.E., BRIK M.G., BROWN E. & HOMMERICH U. J. (2009): Synthesis and optical properties of infrared-emitting YF3: Nd nanoparticles. J. Appl. Phys. 106, 063118.

VON MALTZAHN G., PARK J.H., AGRAWAL A., BANDARU N.K., DAS S.K., SAILOR M.J. & BHATIA S.N. (2009): Computationally guided photothermal tumor therapy using long-circulating gold nanorod antennas. Cancer Res. 69, 3892–3900.